

Spatial Resolution Enhancement of Terrestrial Features Using Deconvolved SSM/I Microwave Brightness Temperatures

Michael R. Farrar and Eric A. Smith

Abstract—A method for enhancing the 19, 22, and 37 GHz measurements of the SSM/I (Special Sensor Microwave/Imager) to the spatial resolution and sampling density of the high resolution 85-GHz channel is presented. An objective technique for specifying the tuning parameter, which balances the tradeoff between resolution and noise, is developed in terms of maximizing cross-channel correlations. Various validation procedures are performed to demonstrate the effectiveness of the method, which hopefully will provide researchers with a valuable tool in multispectral applications of satellite radiometer data.

I. INTRODUCTION

Due to the limited size of satellite instrument antennas and the very low levels of microwave energy emanating from the earth-atmosphere system, it has been required that orbiting instruments measure this radiation with large fields of view (FOV's) or large "effective" apertures. This feature is necessary to ensure an adequately high signal-to-noise ratio (SNR). As these requirements differ for each SSM/I frequency, this, by necessity, results in differing ground footprints for each frequency, as illustrated in Fig. 1. For example, at the 3-dB levels used for the SSM/I instrument, the 19 GHz channel ground footprint is 69 km \times 43 km, while the size for 85 GHz is only 15 km \times 12 km.

When utilizing measurements at different frequencies in multichannel retrievals or other objective modeling applications, it is desirable that the measurements be collocated in time and space. Identical antenna boresights for each respective satellite channel (or identical central points of the ground footprints) do not guarantee spatial collocation as channels with larger fields of view sample larger surface areas. For example, a specific SSM/I 19 GHz measurement may sample a small but significant feature such as a thunderstorm, whereas this feature may effectively lie outside of the FOV of the 85 GHz measurement. Hence comparisons of these measurements at multiple frequencies are hampered by the fact that different phenomena are being sampled by different channels. Therefore, uniform spatial resolution is desired for multichannel applications.

Manuscript received June 1, 1991; revised September 26, 1991. This work was supported by NASA Grant NAGW-991. A portion of the computing resources were provided by the Supercomputer Computations Research Institute at Florida State University under DOE Contract FC058ER250000.

The authors are with the Department of Meteorology and Supercomputer Computations Research Institute, The Florida State University, Tallahassee, FL 32306.

IEEE Log Number 9105689.

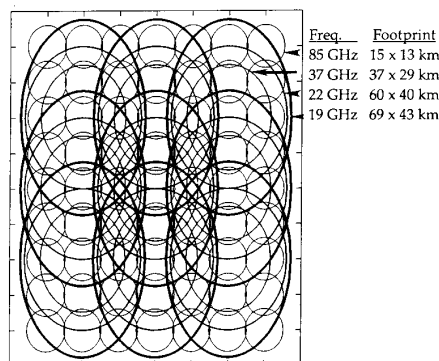


Fig. 1. Ground footprint overlap of the four SSM/I frequencies.

This requirement poses a dilemma. One must either effectively average the high resolution measurements down to the scale of the low resolution, or alternatively attempt to improve or enhance the low resolution measurements up to that of the high resolution. As the former results in the loss of smaller scale information, the latter is obviously preferred. The optimal methods for increasing spatial resolution rely on an overlap of the gain functions of adjacent antenna measurements. This redundancy of information makes it possible to retrieve information, namely, deconvolved brightness temperatures, on scales smaller than those directly sensed by the antenna.

The correction technique presented utilizes a matrix inverse method proposed by Backus and Gilbert [1] and applied by Stogryn [2] to the problem of satellite radiometric measurements. Essentially when the density of such measurements is oversampled, the redundancy in the measurements coupled with the antenna gain pattern of the sampling instrument may be combined to produce a set of coefficients, which when applied to measurements surrounding a central point, can produce a data set whose spatial resolution is greater than the original data. Since Backus and Gilbert showed that such an attempt to enhance resolution leads to an amplification in noise, Stogryn proposed a method which simultaneously works to enhance resolution and minimize noise, where these two properties are balanced by a tuning parameter.

Poe [3] proposed a method by which the low density measurements of the SSM/I lower frequencies were resampled to the higher grid density of 85 GHz. As no attempt was made to increase the spatial resolution of the resampled measurements,

the problem of minimizing noise could be neglected. Although this method is quite useful in such applications as imaging, the problem of inequality in spatial sampling between channels is not addressed. This paper seeks a solution to this problem by attempting to increase the spatial resolution and sampling rate of the low resolution SSM/I measurements to that of the high resolution 85 GHz channel. By a careful objective selection of the tuning parameter within Stogryn's theoretical framework, a method is developed which enhances the SSM/I channels to a common resolution, which may prove to be valuable in multispectral applications of satellite data.

II. METHOD OF SOLUTION

Various methods have been employed by researchers to describe brightness temperatures of specified regions in terms of measured antenna temperatures. Most attempts which have tried to increase resolution have also had the undesirable side effect of amplifying noise in the measured data. Stogryn [2] recognized that the problem of inverting a series of antenna temperatures to yield a brightness temperature was mathematically identical to that of inverting antenna temperatures (measured in either the microwave or infrared regime) to yield an atmospheric temperature profile. Research in this field had already shown that attempting to obtain higher resolution in the retrieved profiles could result in the amplification of noise. This trade-off between noise and resolution was recognized by Backus and Gilbert [1] in their geophysical research. Stogryn's [2] application of the Backus-Gilbert matrix inverse method to the problem of estimating brightness temperatures seeks to circumvent noise amplification by the use of a tuning parameter. We have implemented the technique in conjunction with SSM/I measurements in such a fashion so as to objectively determine the tuning parameter. A discussion of the method follows.

Following Stogryn [2], consider a satellite-borne radiometer observing the earth-atmosphere system from a known altitude (h) and boresight direction (\hat{s}_0) as illustrated in Fig. 2. The incremental solid angle viewed by the antenna may be described as:

$$d\Omega = (-\hat{s} \cdot \hat{\rho}/s^2) dA \quad (1)$$

where $\hat{\rho}$ is the unit vector along a position vector from earth center to the incremental surface area dA , (\hat{s}) is the unit vector from the antenna to area dA , and s is the distance from the antenna to dA . Therefore, the antenna temperature (T_A) measured along the boresight direction may be expressed in terms of an integration of the antenna gain function (G) over the observed brightness temperature field (T_B):

$$\begin{aligned} T_A(\hat{s}_0) &= \int_E G(\hat{s}_0, \hat{s}) T_B(\rho, \hat{s}) d\Omega \\ &= \int_E G(\hat{s}_0, \hat{s}) T_B(\rho, \hat{s}) (-\hat{s} \cdot \hat{\rho}/s^2) dA \end{aligned} \quad (2)$$

where the integral is evaluated over the portion of the Earth (E) seen by the satellite.

In realizing that this process is not instantaneous but is being performed over a finite period of time, two more

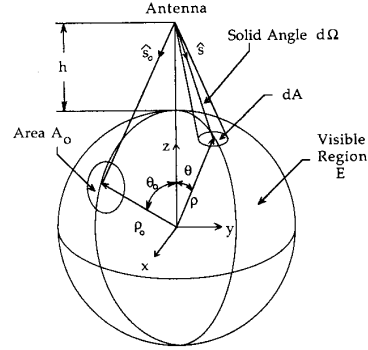


Fig. 2. Geometry for satellite radiometric observations; adapted from Stogryn [2].

aspects of the problem arise. First, the movement of the instrument as it scans and movement of the platform as it orbits the Earth must be considered. This may be dealt with by allowing the appropriate quantities in (2) to become functions of time. Secondly, the integration or measurement time of the instrument itself must be taken into account. This may be accomplished by considering the antenna temperature averaged over the integration time T . Allowing for these two time dependencies leads to:

$$T_A = \frac{1}{\tau} \int_{t_i - \tau/2}^{t_i + \tau/2} \int_E G(\hat{s}_0(t), \hat{s}(t)) T_B(\rho, \hat{s}(t)) (-\hat{s}(t) \cdot \hat{\rho}/s^2(t)) dA dt. \quad (3)$$

However, the observed brightness temperature field varies little during the integration time of the instrument ($\tau < 8\text{ms}$). By neglecting the variation in T_B over the integration time τ , we may describe the i th value of a time-averaged antenna temperature T_{A_i} as:

$$T_{A_i} = \int_E \bar{G}_i(\rho) T_B(\rho) dA \quad (4)$$

where all the time variation has been explained by the time-averaged gain function:

$$\bar{G}_i(\rho) = \frac{1}{\tau} \int_{t_i - \tau/2}^{t_i + \tau/2} G(\hat{s}_0(t), \hat{s}(t)) (-\hat{s}(t) \cdot \hat{\rho}/s^2(t)) dt. \quad (5)$$

Consider now that a set of N measurements whose antenna patterns overlap are to be utilized to determine the brightness temperature for some point at ρ_0 on the Earth's surface. As this problem is mathematically identical to that considered by Backus and Gilbert, Stogryn applied their method of solving a system involving a linear combination of the N measurements which approximates $T_B(\rho_0)$:

$$\begin{aligned} T_B(\rho_0) &= \sum_{i=1}^N c_i T_{A_i} \\ &= \int_E \left[\sum_{i=1}^N c_i \bar{G}_i(\rho) \right] T_B(\rho) dA \end{aligned} \quad (6)$$

where a substitution for T_{A_i} has been made from (4). As it is not possible to produce a set of coefficients c_i which yield a

perfect solution for $T_B(\rho_0)$, the problem is reduced to finding a set of coefficients which most closely produces the resultant brightness temperature.

By considering an integral of the form:

$$Q_R = \int \left[\sum_{i=1}^N c_i \bar{G}_i - F(\rho, \rho_0) \right]^2 J(\rho, \rho_0) dA \quad (7)$$

and a normalization constraint:

$$\int \sum_{i=1}^N c_i \bar{G}_i dA = 1 \quad (8)$$

then by appropriate choice of F and J , Q_R can be minimized. The F and J functions are chosen according to a particular application. J is a "penalty" function which allows emphasis to be placed on desired regions in the integration. In an example explained by Poe [3], a case where the gain function displays undesirable sidelobe levels could be handled by selecting a form for J which emphasizes the sidelobes. However, for the application presented here, J is set to unity ($J = 1$). F is chosen to be equal to a constant value of $1/A_0$ within the area A_0 and equal to zero outside this area. The impact of such a choice is such that the minimization of (7) will yield the best estimate of the average brightness temperature over the specified area A_0 . Other criteria for selection of these functions may be used, some of which are discussed by Stogryn [2].

Another aspect affecting the procedure is the propagation of instrument noise into the desired solution of the brightness temperature. As the variance of this random noise is equal to $(\Delta T_{rms})^2$, the variance in the resultant solution of the brightness temperature is

$$Q_N = \vec{c}^T E \vec{c} \quad (9)$$

where \vec{c} is the vector with elements c_i and E is the error covariance matrix. As the noise in this case is purely random and hence no correlation exists between successive measurements, E is a diagonal matrix whose diagonal elements are $(\Delta T_{rms})^2$. In order to ensure a minimum propagation of noise to the solution, (9) could be minimized with the normalization constraint of (8).

The method utilized in this research attempts to balance the trade-off of resolution and noise, with the constraint of (8), by minimizing the combination of Q_R and Q_N , i.e.,

$$Q = Q_R \cos \gamma + w Q_N \sin \gamma \quad (10)$$

where w is chosen to insure that Q_R and Q_N are dimensionally consistent and the tuning parameter γ allows emphasis to be placed on resolution or noise as it is varied from 0 to $\pi/2$, respectively.

Having defined the minimization problem, the solution may be now be expressed. Allow G to be the $N \times N$ matrix with elements:

$$G_{ij} = \int \bar{G}_i(\rho) \bar{G}_j(\rho) dA. \quad (11)$$

Then the solution vector \vec{c} becomes

$$\vec{c} = Z^{-1} \left[\cos \gamma \vec{v} + \frac{1 - \cos \gamma \vec{u}^T Z^{-1} \vec{v}}{\vec{u}^T Z^{-1} \vec{u}} \vec{u} \right] \quad (12)$$

where

$$\begin{aligned} \vec{u}_i &= \int \bar{G}_i(\rho) dA \\ \vec{v}_i &= \int \bar{G}_i(\rho) (1/A_0) dA \\ Z &= \cos \gamma G + w \sin \gamma E. \end{aligned} \quad (13)$$

The solution of (12) in conjunction with (6) and the specification of G yields the solution for $T_B(\rho_0)$.

III. IMPLEMENTATION OF SOLUTION FOR SSM/I

Once the deconvolution method has been developed, several specific characteristics of the measuring instrument and scan geometry must be incorporated to uniquely specify the problem. One aspect of this problem is the number of neighboring measurements that can be used in the inversion. As the SSM/I employs a conical scanner, which causes the orientation of neighboring footprints to be different for each position along a scan line, the choice of a constant number of footprints for all scan positions is undesirable. The criterion thus chosen was one of proximity, such that all footprints whose center points lie within a specified elevation from the boresight would be considered. An elevation cutoff value of 1.5° is selected in attempt to balance a trade-off. The gain at this elevation drops by approximately an order of magnitude for 19 GHz (by two orders of magnitude for 37 GHz), while the gains at smaller elevations would still have relatively large values and significant contributions to the measured brightness temperature might be neglected. Conversely, larger values of the elevation cutoff would involve many more measurements and hence slow the calculation process.

Aside from orbital and scanning characteristics, two instrument specifications are needed to implement this method: instrument noise levels and antenna gain patterns for each channel. The error covariance matrix E may now be defined as previously described by assigning to ΔT_{rms} the appropriate values for each channel, as described by Hollinger [4].

As only limited gain information was recorded for the instrument utilized (instrument S/N 002 aboard DMSP F8), some interpolation is necessary for the \bar{G} function. The gain function is determined at a resolution of 0.1° in elevation angle (displacement from boresight), but only at intervals of 45° in azimuth. In an attempt to produce spatially complete patterns, the gain data are interpolated to a resolution of 0.01° in elevation angle by a cubic spline. Due to the azimuthal symmetry of the patterns, it was found feasible to average over azimuth, yielding gain patterns which are functions of elevation angle only. Fig. 3 depicts the interpolated gain versus the eight azimuthal cuts for the 37 GHz channel (horizontal polarization). The azimuthally averaged gain matches the gain for each azimuthal cut quite well for elevations less than 1.5° , the cutoff value utilized.

The contribution of brightness temperatures away from the boresight to the measurement of the brightness temperature along the boresight is accomplished by taking advantage of the overlapping antenna patterns of neighboring measurements. Hence the gain of each measurement with respect to the

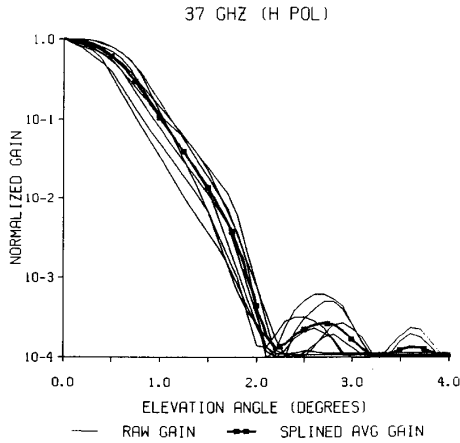


Fig. 3. Raw antenna gain versus azimuthally averaged antenna gain. The raw gain information (calibrated in 45° azimuthal cuts) are depicted by the eight thin lines, contrasted by the azimuthally averaged antenna gain pattern shown in bold.

relative position of its neighbors must be determined. This, in turn, requires a knowledge of the scan geometry in order to describe the relative positions between successive measurements and their ground footprints. As the SSM/I employs a conical scanner, the exact determination of such a geometry leads to computational complexity. However, by making a tangent plane approximation, oriented such that this plane is tangent to the Earth's sphere at the point of intersection of the boresight and the Earth's surface, it is possible to obtain nearly exact results for small displacements away from the boresight. After the displacement of neighboring footprints from the boresight is found in terms of elevation and azimuth, they are matched with the interpolated antenna patterns to yield the appropriate gain values. Once the instrument gain is properly incorporated, the G matrix may be uniquely specified allowing the solution vector \mathbf{c} to be obtained.

IV. OBJECTIVE SPECIFICATION OF THE TUNING PARAMETER

One final parameter remains unaccounted for in the solution vector: the tuning parameter γ , which attempts to balance the trade-off between resolution and noise. As each frequency channel views the same features with differing FOV's, smaller scale features easily distinguishable in the high frequency data are blurred by the large FOV's of the lower frequency channels. Even so, a high correlation is still observed when cross-channel comparisons are made. As the result of the deconvolution procedure will be to match the fields of view of the low frequency channels with that of the 85 GHz channels, smaller scale features blurred in the raw low frequency data are revealed in the enhanced data, which, in turn, will increase the cross-channel correlations. If too high a value of the tuning parameter γ is selected, the FOV will not be adequately narrowed and the increase in cross-channel correlation will be reduced. Likewise, if too low a value of γ is chosen, too much noise will be added to the solution and again the increase in cross-channel correlation will be reduced. Since there is no *a priori* rule which uniquely determines this parameter,

TABLE I
AVERAGE VALUES OF G DETERMINED BY COASTAL
CALIBRATION CASES CHANNEL TUNING PARAMETER (γ)

Channel	Tuning Parameter (γ)
37 GHz (V)	$0.53 \pi/2$
37 GHz (H)	$0.48 \pi/2$
22 GHz (V)	$0.13 \pi/2$
19 GHz (V)	$0.13 \pi/2$
19 GHz (H)	$0.08 \pi/2$

we choose γ on the basis that the intercorrelation between channels is maximized.

A number of test data cases have been analyzed in this fashion to select a set of optimum tuning parameters. In the process, we have avoided the selection of test cases which may lead to negative correlations, such as precipitation. The scattering effects of precipitation-sized particles at the higher frequencies (i.e., 85 GHz) can lead to radiation losses and hence minimum values in the brightness temperatures. However, these same precipitation regions will have little scattering effect at the lower frequencies, and due to emission effects, will, in fact, appear as relative maxima. This negative correlation due to precipitation, when coupled with the remainder of the scene which is positively correlated, contaminates the cross-channel correlation approach in determining optimal tuning parameters.

Another consideration is that there must be sufficiently high brightness temperature gradient information such that the blurring effect of the lower resolution channels is measurable. Such gradients are found along coastlines, where cool ocean brightness temperatures transition rapidly to warm land brightness temperatures. Hence, rain-free coastline cases were chosen to determine the γ 's with the cross-correlation technique. Approximately 100 coastline cases were selected from four ocean basins: Western Pacific, Eastern Pacific, Caribbean, and Indian Ocean coastlines.

After determining the optimum γ at each channel for all the selected coastline cases, the results were averaged to yield a set of coefficients (given in Table I) which could be utilized for general applications. Such applications may include those which require computational speed, as the implementation of such predetermined coefficients avoids the extra computer time required to calculate the optimum values. Another such application is made where the cross-channel correlation technique is not applicable, such as for precipitation cases.

We note that the solutions are dependent on the choice of γ , and that utilization of average γ 's does not always yield the level of detail which can be obtained by the case sensitive approach. Hence there may be no universal best set of γ 's, although the search is still ongoing. In the remainder of this paper, we have only considered applications where the tuning parameter has been determined independently on a case-by-case basis.

V. QUANTITATIVE VALIDATION

The only way to truly validate the resolution enhancement of the SSM/I low frequency channels would be to compare enhanced measurements to those actually made at the

desired high resolution. However, as such high resolution measurements of the SSM/I low frequency channels coincident to their actual low resolution measurements do not exist, such comparisons cannot be made and hence other methods of validation must be pursued. Two forms of quantitative validation were selected to illustrate the effectiveness of the deconvolution method. First, a simple linear regression technique is presented as a standard by which the deconvolution method may be compared. Secondly, a self-consistency test was performed by averaging a high resolution data set to a lower resolution, whereby the deconvolution procedure is invoked on the averaged set in an attempt to retrieve the original high resolution data. As actual high resolution measurements of the SSM/I low frequency channels coincident to the actual measurements do not exist, strict numerical validation of the deconvolution procedure is elusive. Nevertheless the validation tools chosen do illustrate the usefulness of the method. The first way of demonstrating the effectiveness of such a rigorous procedure as the deconvolution method is to show that it can improve on the results of a simpler technique. A linear regression procedure developed by Spencer [5] provides the method of comparison. Spencer performed a linear regression on a set of horizontally polarized 19 GHz brightness temperatures along coastlines to produce a new set of brightness temperatures which most closely matched the horizontally polarized 37 GHz brightness temperature pattern. As this represents the equivalent of an enhancement of 19 GHz brightness temperatures to the resolution of 37 GHz, the deconvolution method was reconfigured to this enhancement for the purpose of comparison. When applied to the 19 GHz brightness temperatures for several cases, the linear regression of Spencer [5] explains 97.95% of the total variance in the 37 GHz data, whereas the deconvolution method explains 98.65% of the variance. This represents a 34.15% quantitative improvement in terms of reducing the unexplained variance. However, even though the deconvolution method leads to an improvement over the linear regression technique, the raw 19 GHz data themselves explained such a high percentage of the variance (over 97%) that such a comparison by itself is not an adequate proof of the superiority of the method.

Thus a self-consistency test was chosen as a second quantitative means of validation. If the high resolution measurements are smoothed to a lower resolution, a proper enhancement procedure performed on the smoothed data should yield an enhanced data set very close to the original high resolution data. This self-consistency approach was performed on several sets of 85 GHz vertically polarized brightness temperatures to numerically validate the deconvolution method. First, the 85 GHz data were subjected to the same deconvolution procedure as previously described, with two exceptions. Whereas before the resolution of the low frequency channels had been increased utilizing their respective gain functions, here the resolution has been reduced to that of 37 GHz utilizing the gain function of the 85-GHz instrument. Secondly, as the act of smoothing inherently reduces noise, the consideration of noise reduction in the procedure can be neglected by choosing a zero value for the tuning parameter ($\gamma = 0$). The smoothed data set was then enhanced back to the 85-GHz

resolution as originally described, where it was compared with the original data in terms of an rms difference. For a perfect enhancement with no noise production, such a comparison should result in an rms difference between the original data and the smoothed/reenhanced data of no more than the inherent noise of the instrument. The average rms difference for the series of 85-GHz vertically polarized test cases was 1.47 K, roughly twice the value of 0.75 K reported by Hollinger [4] as the noise inherent in the 85-GHz instrument. Hence the enhancement process only generates approximately 0.75 K of added noise. Note that the smoothing and enhancement processes differ in their choices of gain functions, limits of spatial integration, and selection of the tuning parameter. Thus their implementations are independent and are not merely an inversion of one another. Hence this validation approach is not simply a measure of how well the matrix processes can be inverted but is instead a legitimate estimate of the effectiveness of the enhancement procedure.

VI. QUALITATIVE GEOGRAPHICAL VALIDATION

If the procedure is truly improving the spatial resolution of the measurements, prominent geographical features should be enhanced in the resultant images. Thus a qualitative validation procedure has been applied for a number of geographical cases to reinforce the conclusions of the previous section. Such a case for the Caribbean basin and Florida peninsula is presented in Fig. 4, where (a) a raw 19-GHz image (a) and an enhanced image (b) are presented for comparison. Whereas the actual raw measurements blur the boundary between land and ocean and hence underestimate the brightness temperatures of the land along the coast, the deconvolved data not only enhances the resolution but tightens this coastal brightness temperature gradient. This blurring effect is especially noticeable in many Caribbean islands, where due to their small size, the brightness temperatures are smeared not only along the coastlines but throughout the interiors as well. The deconvolution procedure improves on the coastlines and actually increases the brightness temperature values of the relatively warmer and drier island interiors, most dramatically illustrated in the depiction of Cuba, Andros, Jamaica, and Hispaniola. The process also works in the other direction so as to enhance a relative minimum, as illustrated by Lake Okeechobee (in south Florida). Whereas the raw image of the lake is blurred with the surrounding warmer land, the deconvolved image enhances the boundaries while producing a lower brightness temperature for the relatively colder lake waters.

Another such case for the western coast of India is illustrated in Fig. 5. As for the Caribbean case, the deconvolution procedure better defines the coastal brightness temperature gradient. When compared to a geographical map as illustrated in Fig. 6, the deconvolution procedure enhances the Indian coastline to a resolution which better matches the actual geographic features. What is most notable is the improvement of the actual geographic coastline, depicted by the enhanced definition of the Gulfs of Kutch and Khambhat along with the peninsula of Gujarat that lies between. Whereas this peninsula is blurred by the raw image, the deconvolved image actually

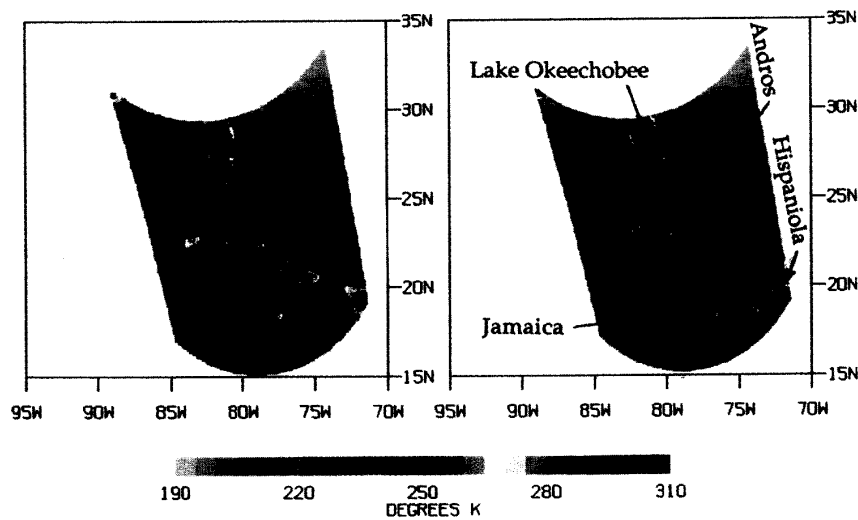


Fig. 4. Raw versus deconvolved 19-GHz image of Caribbean basin and Florida peninsula.

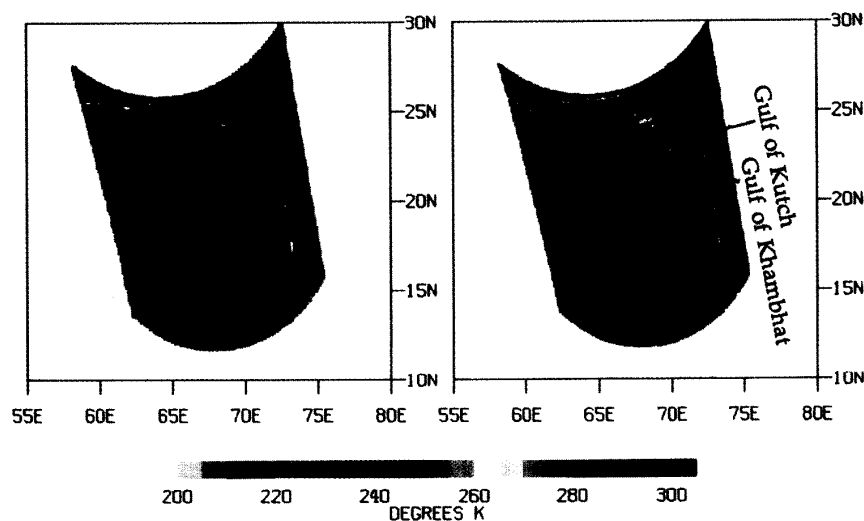


Fig. 5. Raw versus deconvolved 37-GHz image of the western Indian coastline.

matches the geographic pattern, highlighted by the shape of the tip of the peninsula, near the city of Okha (located by * in Fig. 6). In addition to the two examples shown, many more cases were examined to determine the effectiveness of the method in improving the geographic details of the scenes. The deconvolution method was found to consistently tighten the coastal brightness temperature gradients, bring out small features blurred by the raw data, and better depict actual geographic features.

VII. CONCLUSIONS

A deconvolution method for enhancing low frequency SSM/I brightness temperatures utilizing the Backus-Gilbert

matrix inversion technique has been presented. The opposing effects of resolution enhancement and noise production have been balanced by an objective selection of the tuning parameter based on maximizing cross-channel correlations. The effectiveness of the procedure has been demonstrated through various quantitative and qualitative validation tests. The method offers researchers spatially consistent, multifrequency data at an enhanced resolution for a variety of remote sensing applications in which spatial coherence among measurements is desired.

ACKNOWLEDGMENT

The authors wish to thank Gene Poe, Richard Savage, Roy Spencer, and Jim Hollinger for their generosity and

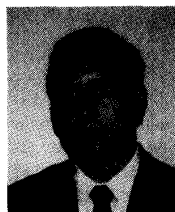


Fig. 6. Geographical map of western India. The city of Okha at the tip of Gujarat is indicated by an asterisk (*).

assistance. Their contribution of SSM/I technical information and their valuable time in personal communications was greatly appreciated. The authors also thank Jim Merritt for his capable assistance in software development and imaging analysis.

REFERENCES

- [1] G. Backus and F. Gilbert, "Uniqueness in the inversion of inaccurate gross earth data," *Phil. Trans. Roy. Soc. London*, vol. A266, pp. 123-192, Mar. 1970.
- [2] A. Stogryn, "Estimates of brightness temperatures from scanning radiometer data," *IEEE Trans. Antennas Propagat.*, vol. AP-26, pp. 720-726, Sept. 1978.
- [3] G. A. Poe, "Optimum interpolation of imaging microwave radiometer data," *IEEE Trans. Geosci. Remote Sensing*, vol. GE-28, pp. 800-810, Sept. 1990.
- [4] J. Hollinger, "DMSP Special Sensor Microwave/Imager calibration/validation. Final Report, Volume 1," Naval Research Laboratory, Washington, DC, July 1989.
- [5] R. Spencer, personal communication, 1990.



Michael Farrar was born in Nashville, TN on June 24, 1964. He graduated from Purdue University in May 1986 with the B.S. degree in physics, at which time he was also commissioned as a 2nd Lt. in the U.S. Air Force. He then went to Penn State University, where he received the B.S. degree in meteorology in May 1987. He was then assigned to Headquarters, U.S. Air Forces Europe (USAFE), Ramstein AB, Germany, where he served as a forecaster and command briefer until July, 1989. Upon his return to the U.S., he then enrolled at

Florida State University in order to pursue the Master's degree in meteorology. Since then he has been conducting research into SSM/I resolution improvement and its impact on remote sensing applications, most notably rainfall retrieval. He currently holds the rank of Captain, and will serve at the Scientific Services Division of 3rd Weather Wing at SAC Headquarters, Offutt AFB, NE, following his graduation in August 1991.



Eric A. Smith was born in West Palm Beach, FL on July 16, 1943. He received the B.S. degree in mathematics in 1966 from the University of Wisconsin and the M.S. and Ph.D. degrees in atmospheric science in 1980 and 1984 from Colorado State University.

He engaged in research at the University of Wisconsin's Space Science and Engineering Center until 1975. During this period he developed an interactive-correlative technique for estimating the wind field from time sequences of analytically navigated geosynchronous satellite images which has been widely applied in the framework of interactive McIDAS systems, of which he was one of the developers and original author. From 1975 to 1984 he was a research scientist at Colorado State University. There he conducted research in satellite meteorology and design of solid state image processing systems (ADVISAR). His research at CSU included studies of cloud size and optical thickness; cloud top height; bispectral cloud retrieval techniques; multispectral analysis of visible infrared, and microwave data; satellite estimation of cloud cover distribution and radiation budget parameters; diurnal variation of tropospheric cloud-radiation processes; earth radiation budget; solar variability; and satellite precipitation estimation. He is presently a professor in The Department of Meteorology and Supercomputer Computations Research Institute (SCRI) at The Florida State University. His present research at Florida State University is directed in three areas: 1) the radiative energetics of the Southwest Monsoon System and the desert heat low regimes over the Arabian Peninsula, the western Gobi desert, and the Tibet Plateau; 2) the global radiation budget, cloud-radiative forcing and feedback, and surface energy budget physics based on satellite observations and biophysical modeling; and 3) microwave radiative transfer modeling and precipitation retrieval from passive microwave satellite measurements.